

ARCTIC SEA ICE VARIABILITY AND TELECONNECTIONS WITH CLIMATE INDICES: A WAVELET ANALYSIS APPROACH

Under Guidance of
Dr.R.Maheswaran

>>>

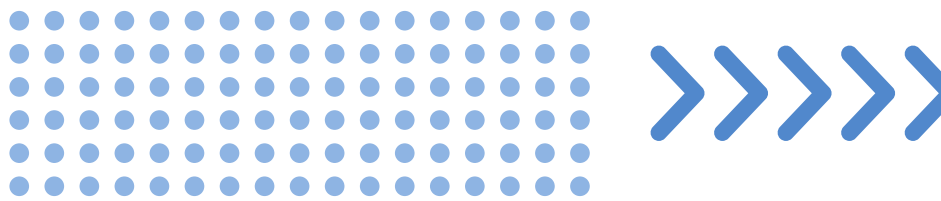
Baipilli Naveen-CC24MTECH11006
Menda.Saranya-CC24MTECH11007



Introduction



- The sea ice cover is one of the key components that has been a focus of attention in recent years, largely because of a strong decrease in the Arctic sea ice cover.
- The study highlights the significant impact of seasonal, interannual, and decadal variations in Arctic sea ice on the global climate system .
- It emphasizes the uniqueness of Arctic ice formation and variability due to its geographical configuration.
- Changes in Arctic sea ice are linked to climate patterns and weather events across the Northern Hemisphere through a process called atmospheric teleconnection. These include well-known climate modes such as ENSO and the North Atlantic Oscillation (NAO), which can influence everything from European winters to Asian monsoons.



Study Area

The study area encompasses the Arctic Ocean and surrounding marginal seas where seasonal and perennial sea ice occurs. Geographically, it includes regions north of approximately 60°N latitude, covering key basins such as the Beaufort Sea, Chukchi Sea, East Siberian Sea, Laptev Sea, Kara Sea, Barents Sea, and the Central Arctic Basin. This region is characterized by extreme climatic conditions, persistent cold temperatures, and dynamic sea ice variability influenced by atmospheric and oceanic processes. The spatial extent of the study area was defined using a georeferenced image from the National Snow and Ice Data Center (NSIDC), ensuring accurate representation of the typical sea ice domain. The resulting shapefile was used to extract and analyze sea ice concentration data within this boundary.

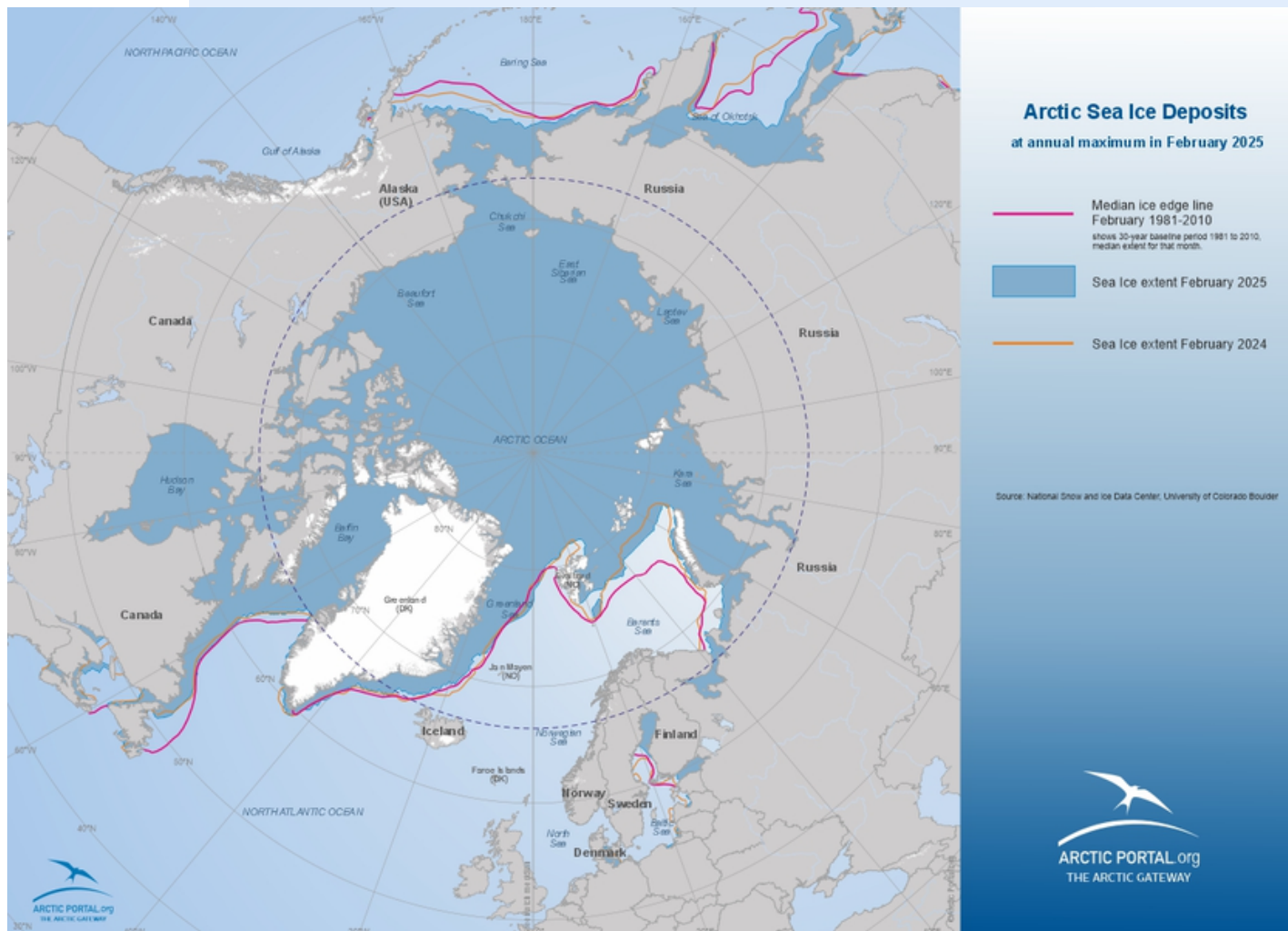


Motivation

According to data from the [National Snow and Ice Data Center \(NSIDC\)](#), the average sea ice extent for the month was 13.75 million square kilometers (5.31 million square miles)—the lowest February extent recorded in the 46-year satellite record.

September 2012

- ▼ Lowest Arctic sea ice extent ever recorded.



What Arctic Ice Loss Means for the World

Sea ice plays a crucial role in regulating global temperatures by reflecting sunlight back into space. As the ice diminishes, darker ocean waters absorb more heat, accelerating warming—a feedback loop known as Arctic amplification

Wavelet-based techniques (CWT, XWT, coherence) offer powerful tools to analyze non-stationary relationships and time-frequency dynamics between sea ice and climate oscillations.

Why wavelet approach?



- Fourier Transform gives only frequency information — you know what periodicities exist, but not when they occurred.
- Wavelet Transform tells you both: What frequency; When that frequency was active
- Handles Non-Stationarity
- Sea ice concentration and climate indices are non-stationary, meaning their statistical properties (mean, variance, periodicity) change with time fourier analysis assumes stationarity — not suitable for shifting climate dynamics.
- Wavelet analysis adapts to local changes in frequency and amplitude.

Like a magnifying glass that moves through time and shows how sea ice concentration variability is linked to climate indices at different timescales and time periods.

CONTINUOS WAVELET TRANSFORM



CWT takes a time series signal and breaks it down into its time and frequency components simultaneously.

1. Choose a Wavelet (Mother Wavelet)
2. Scale the Wavelet to analyse different frequency bands of the signal & slide the wavelet across the entire time axis of signal helps to locate where in time certain frequencies appear
3. We compute the Wavelet Coefficients which shows how much the signal “resembles” the wavelet at each scale a and position b

$$\psi_{a,b}(t) = \frac{1}{\sqrt{|a|}} \psi \left(\frac{t-b}{a} \right)$$

$$W(a, b) = \int_{-\infty}^{\infty} x(t) \cdot \psi_{a,b}^*(t) dt = \frac{1}{\sqrt{|a|}} \int_{-\infty}^{\infty} x(t) \cdot \psi^* \left(\frac{t-b}{a} \right) dt$$

Sum (integral) over all time of the signal multiplied by scaled and shifted versions of the wavelet function.

4. This measures the correlation between $x(t)$ and the scaled/shifted wavelet

CROSS WAVELET TRANSFORM



Cross Wavelet Transform compares two time series in both time and frequency space.

It identifies regions in time-frequency space where both time series show high common power and analyzes the phase relationship between them.

$W^x(a, b)$: CWT of $x(t)$

$W^y(a, b)$: CWT of $y(t)$

1. Given Two Time Series $x(t), y(t)$

2. Cross Wavelet Transform (XWT) Formula This captures the common power and phase relationship between x and y

$$W^{xy}(a, b) = W^x(a, b) \cdot (W^y(a, b))^*$$

3. The cross wavelet power is the magnitude of the cross wavelet transform shows where both time series have high amplitude at the same time and scale.

$$|W^{xy}(a, b)| = |W^x(a, b)| \cdot |W^y(a, b)|$$

4. The phase angle between the two time series is tells which signal is first and which one follows it between $x(t)$ and $y(t)$ at a given scale and time.

$$\phi^{xy}(a, b) = \arg(W^{xy}(a, b))$$

WAVELET TRANSFORM COHERENCE



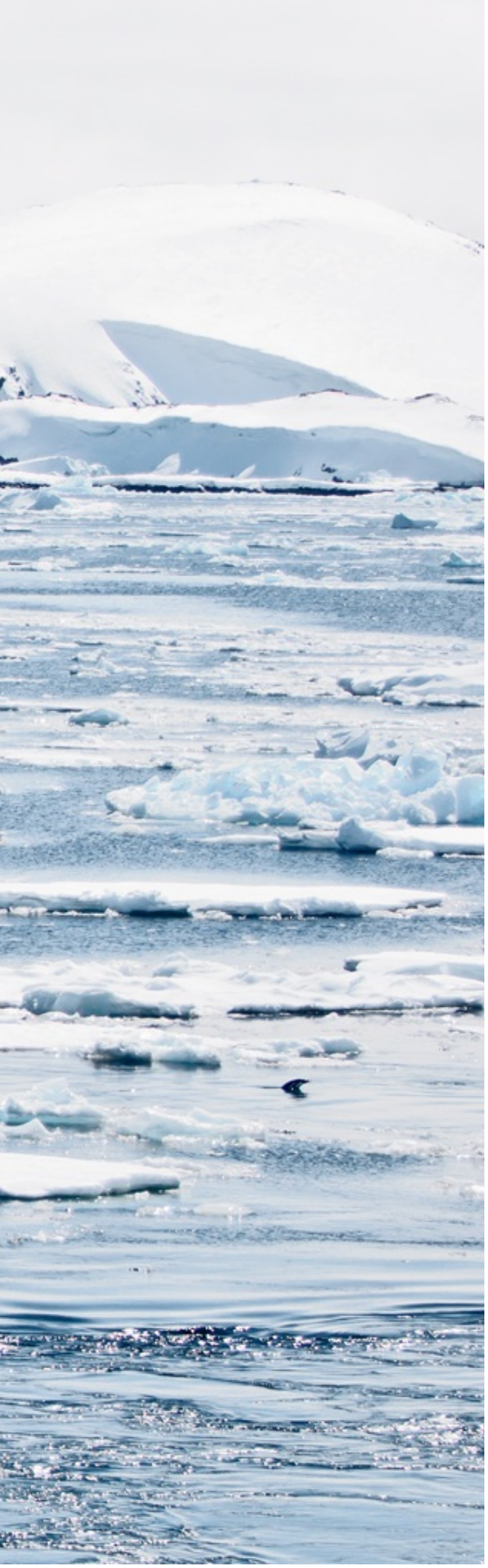
- XWT - power (amplitude) but not whether the relationship is statistically strong here WTC normalizes XWT to detect significant relationships, even if amplitudes are low

$$R^2(a, b) = \frac{|\mathcal{S}(W^{xy}(a, b))|^2}{\mathcal{S}(|W^x(a, b)|^2) \cdot \mathcal{S}(|W^y(a, b)|^2)}$$

Numerator measures how much power the two signals have at the same time and frequency.
Denominator computes the product of the individual wavelet powers

Normalizes the numerator — like dividing the covariance by the product of standard deviations in correlation.

Literature Review



The Arctic was divided into eight regions. The researchers combined sea ice concentration (SIC) and sea ice thickness (SIT) datasets from ESA CCI from 2002 to 2017. Linear regression-SIC & SIT data- seasonal and interannual trends. Mann-Kendall test - detect abrupt changes in SIT

Zongliang Wang(2020)

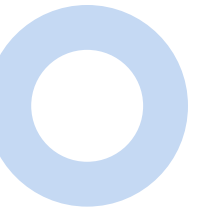
Over the past 42 years, they observed an overall expansion in the total Southern Ocean sea ice extent (SIE). Using wavelet coherence analysis (WCA), they identified significant out-of-phase correlations between sea ice variability and large-scale climate indices and examine the interannual and interdecadal variability of sea ice in the Southern Ocean.

M. Swathi,Avinash Kumar,Rahul Mohan(2023)

Yadav et al. (2022)

The study examined seasonal and long-term SIE changes in the Indian Ocean Sector of Antarctica from 1979–2019. They analyzed how sea ice trends respond to ENSO and SAM using satellite observations, ERA5 reanalysis, and statistical + wavelet-based techniques. Using CWT, XWT, and Wavelet Coherence the study captured interannual and decadal-scale variability

Data Aquisition



Sea ice concentration - National Snow and Ice Data Center (NSIDC)
~25°x25 km
Monthly



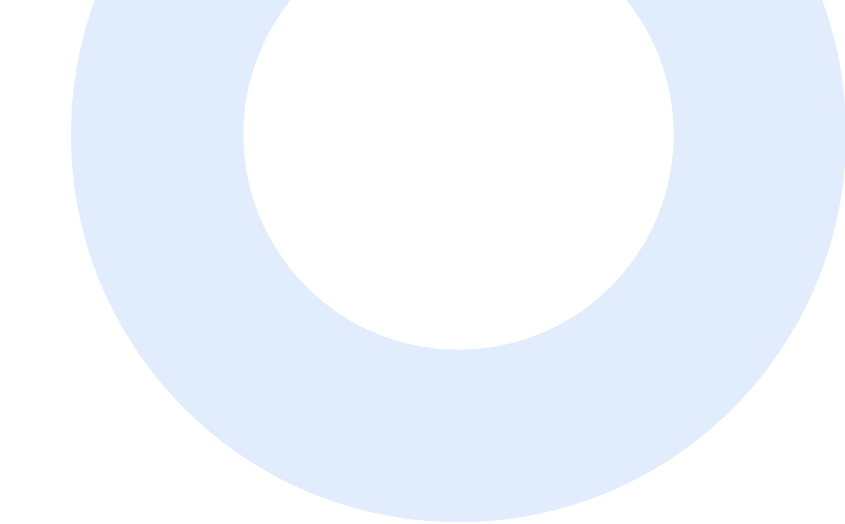
ENSO(Nino 3.4 index), NAO Index , AO Index ----- NOAA



Incoming solar radiation (ERA5)
~0.25° x 0.25° (~31 km)
Hourly - 12 pm



Objectives



Analyze Temporal Trends of Arctic Sea Ice:

Examine long-term trends and seasonal variations in Arctic sea ice concentration using time series plots and statistical trend analysis.



Identify Dominant Periodicities via Continuous Wavelet Transform (CWT):

Apply CWT to detect and characterize the dominant periodic components in sea ice variability, capturing both time and frequency information.



Investigate Time-Frequency Relationships with Climate Indices:

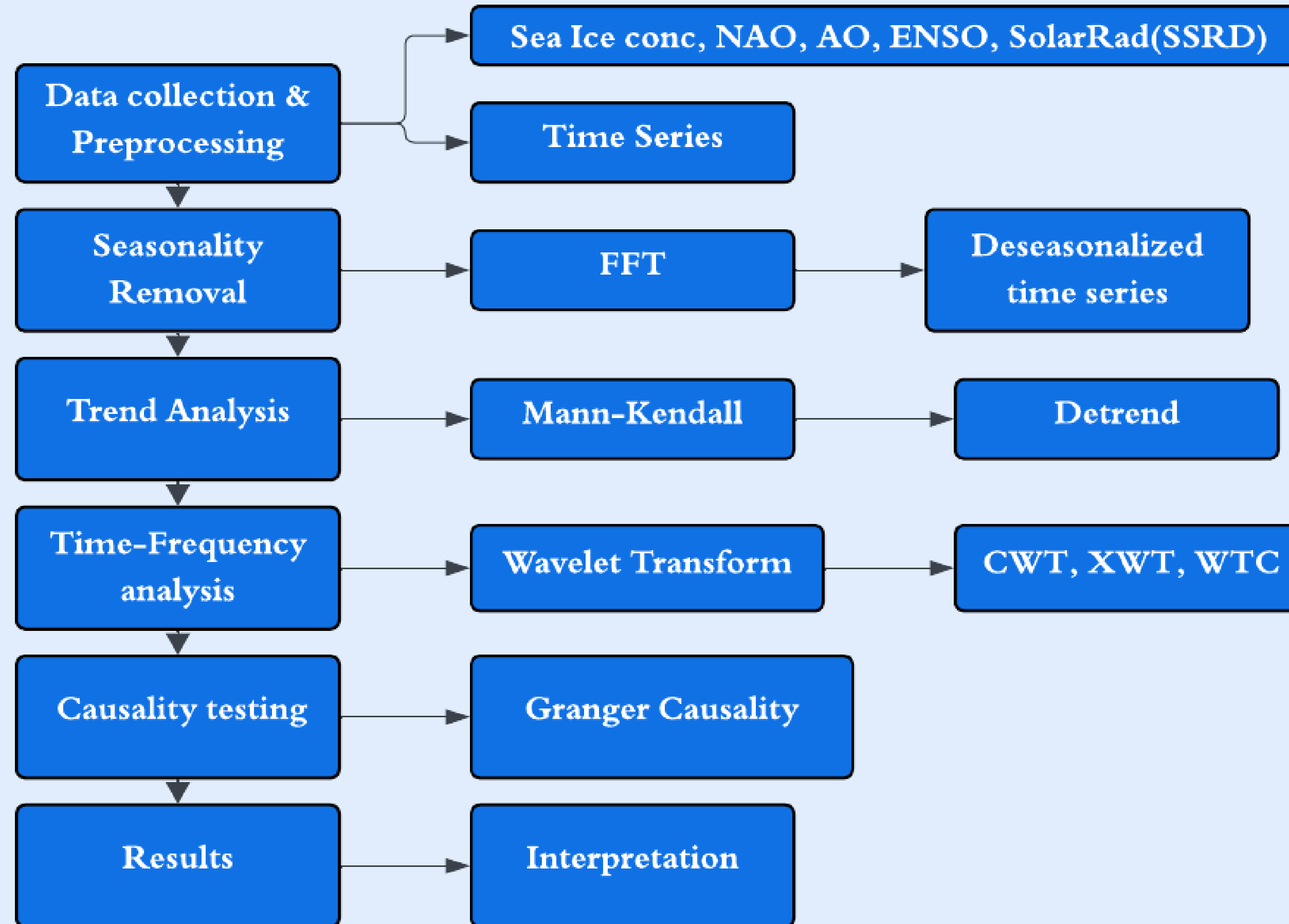
Utilize XWT and Wavelet Coherence to quantify the time-frequency relationships and coherence between Arctic sea ice metrics and major climate indices(ENSO,NAO,AO)



Analyze the identified relationships to understand how large-scale climate modes influence Arctic sea ice concentration



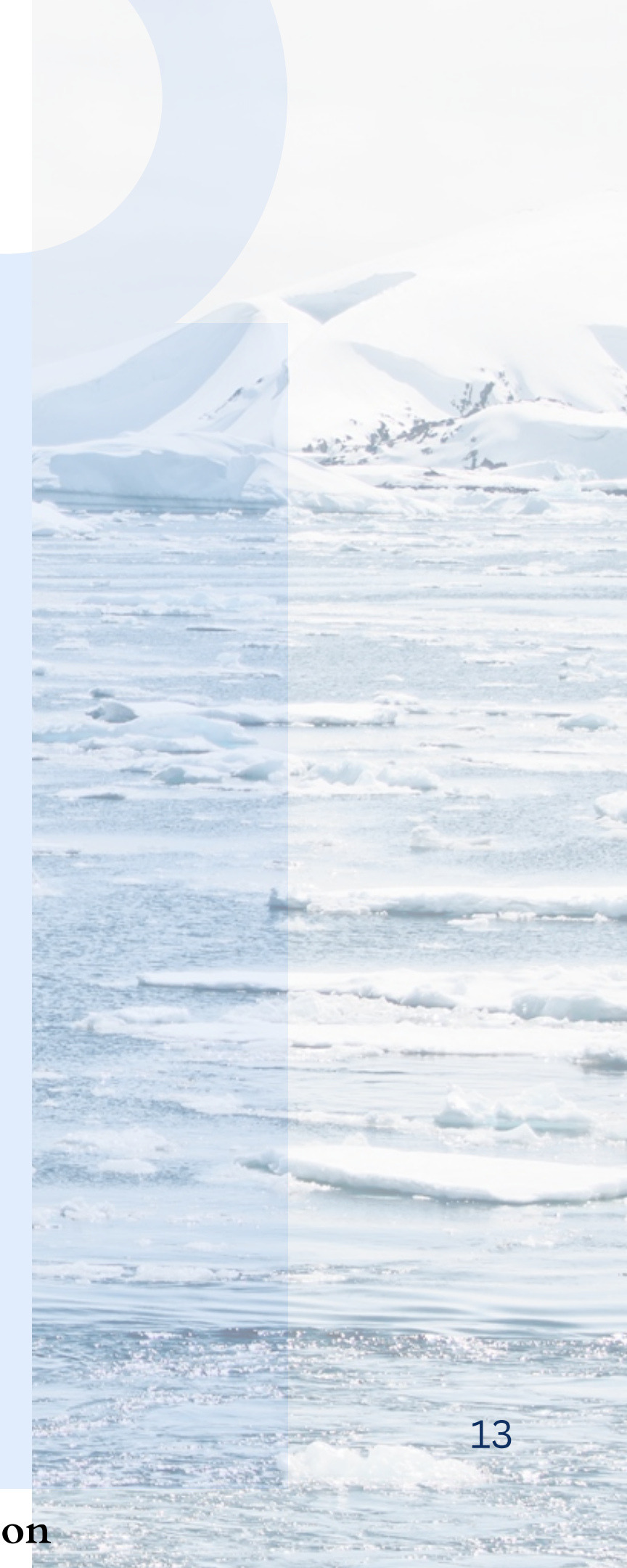
Methodology

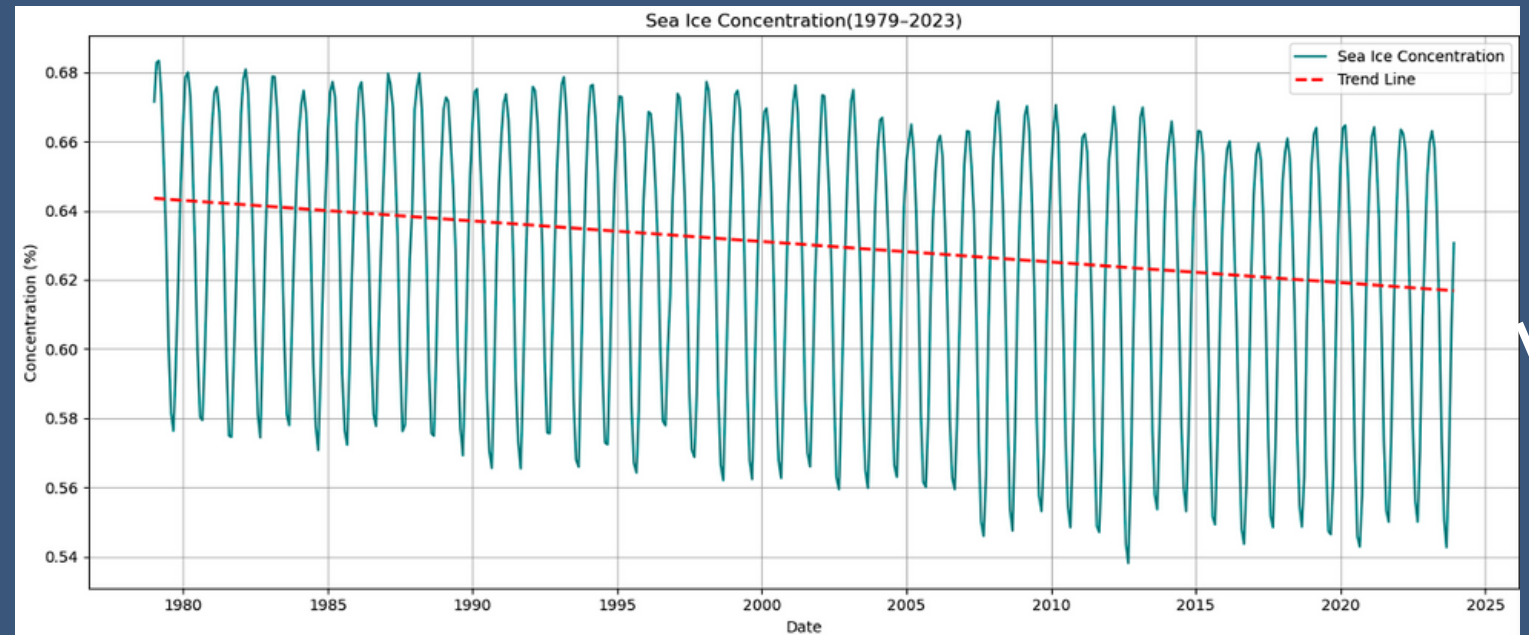


Georeferencing



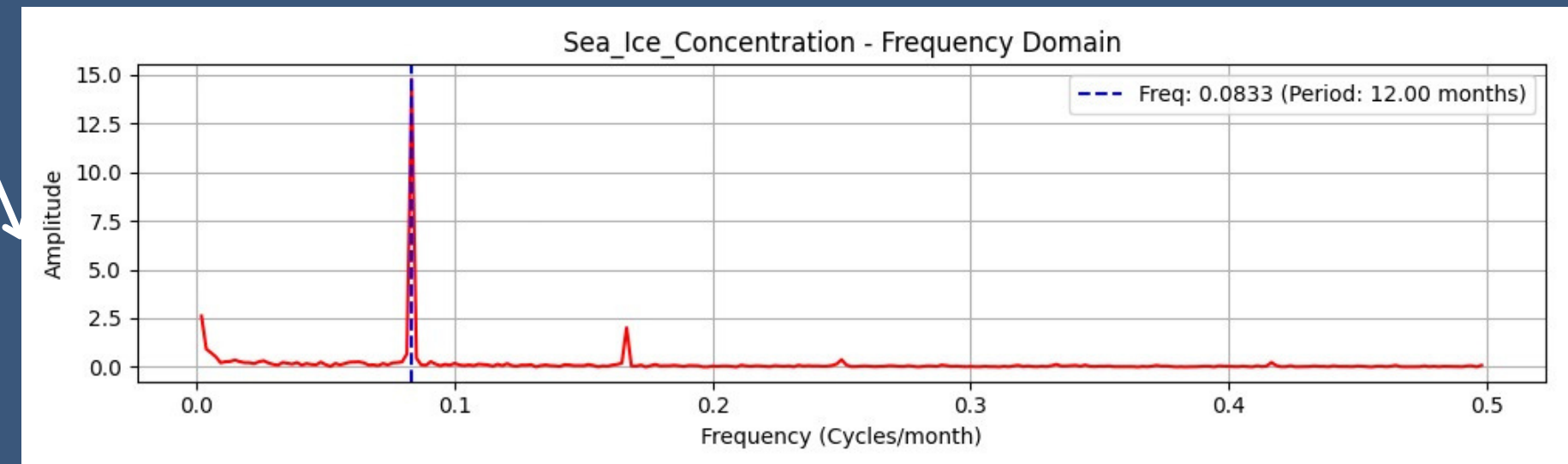
- A reference image showing Arctic sea ice extent was sourced from the National Snow and Ice Data Center (NSIDC) portal.
- A screenshot of the image was taken to use as a base for geospatial referencing.
- The image was imported into a GIS environment (e.g., QGIS/ArcGIS Pro) for georeferencing.
- Control points were assigned based on known latitude and longitude coordinates of identifiable geographic features in the Arctic.
- The image was georeferenced to align with the WGS 84 coordinate system.
- A polygon shapefile representing the Arctic sea ice region was digitized over the georeferenced image.
- This shapefile was used as the spatial boundary for further analysis of sea ice concentration data.





SIC TIME SERIES

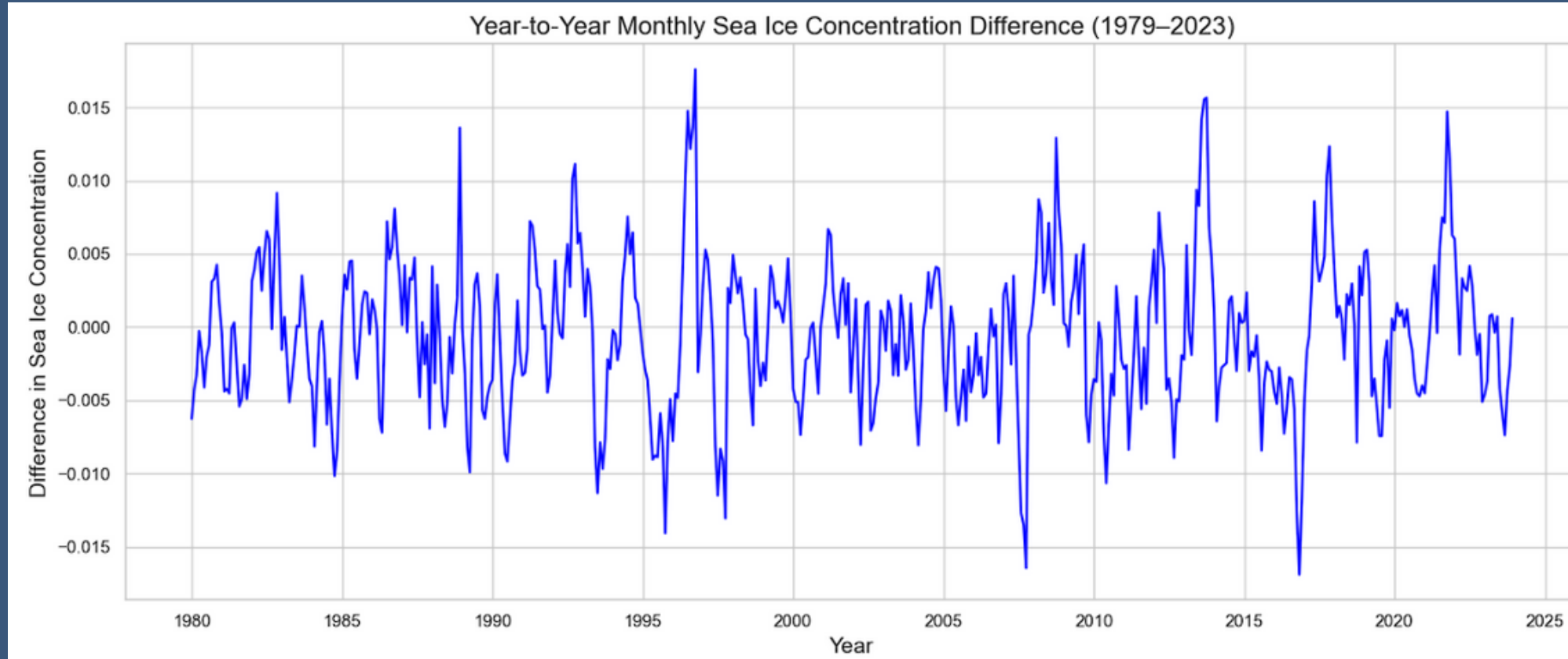
- Seasonal variation due to the annual freeze–melt cycle.
- A decreasing trend – long-term Arctic sea ice decline.



FFT TO SIC TIME SERIES

- Dominant frequency was observed around 12 months i.e, annual cycle

Year-over-Year Differencing Approach



SIC AFTER REMOVING SEASONALITY

To examine the interannual variability in Arctic sea ice while minimizing the influence of the seasonal cycle, we applied a year-over-year differencing method. This technique estimates the change in sea ice concentration (or extent) for each month relative to the same calendar month in the preceding year. Mathematically, this can be expressed as:

$$S(t) = S(t) - S(t - 12)$$

where:

$S(t)$ is the sea ice concentration at month t ,

$\Delta S(t)$ is the differenced value representing the change from the same month in the previous year.

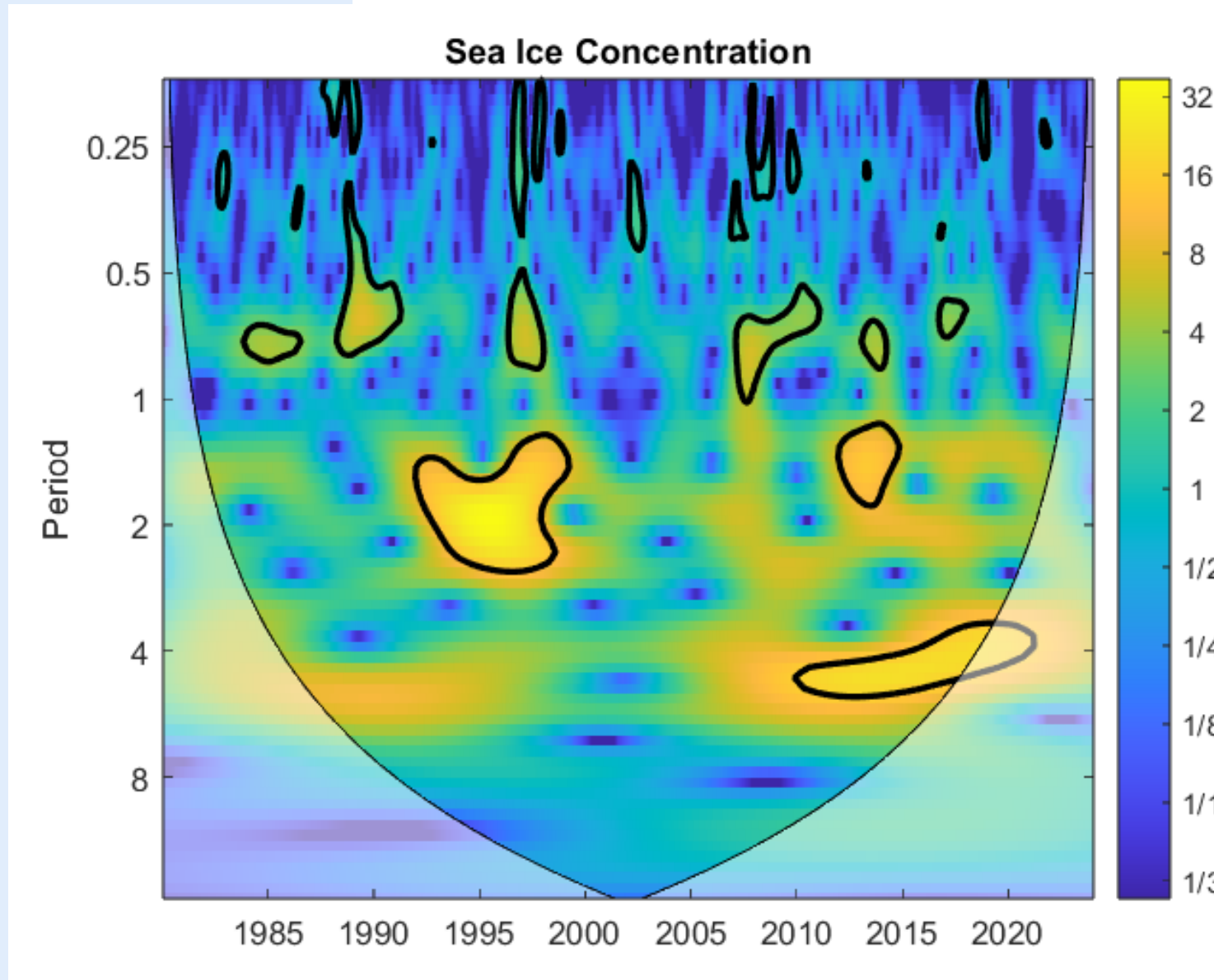
MANN KENDALL TEST

The Mann-Kendall test was applied to both the original and year-over-year differenced sea ice concentration (SIC) data to capture different trend characteristics. The test on the original SIC detects long-term monotonic trends, while the test on the differenced data highlights trends in interannual variability by minimizing seasonal effects. This dual approach provides a clearer understanding of both overall changes in sea ice and shifts in the rate of year-to-year change.

Data Type	Trend	Z-value	p-value	Kendall Tau	Sen's Slope (per year)
SIC	Decreasing	-5.4765	0.0000	-0.1576	-0.000595
SIC After differencing	No trend	0.08173	0.934	0.023	1.17e-07

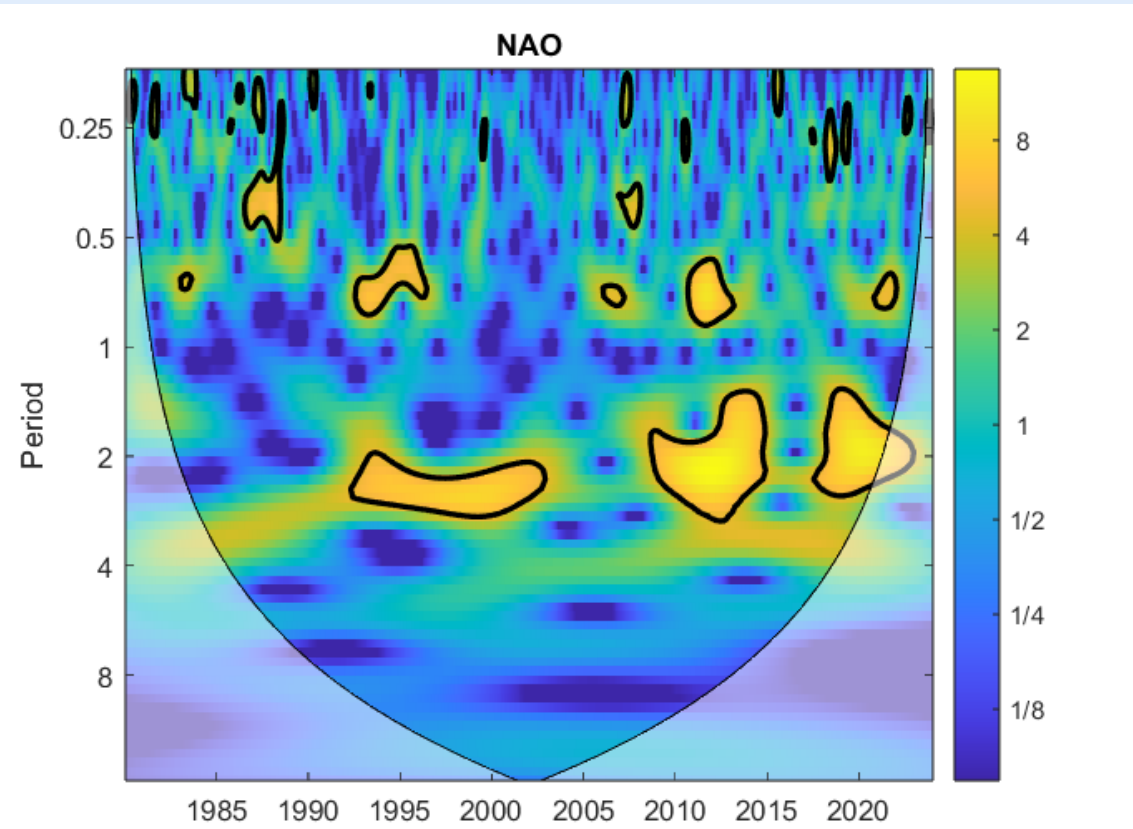
The Mann-Kendall test results indicate a significant long-term decreasing trend in sea ice concentration (SIC) from 1879 to 2023, with a Z-value of -5.4765 and a p-value of 0.0000, confirming the trend's statistical significance. The negative Kendall Tau (-0.1576) and Sen's slope (-0.000595 per year) further support a consistent decline in sea ice over the study period. However, when the test was applied to the year-over-year differenced SIC data—used to remove seasonal effects—no significant trend was detected. The near-zero Z-value (0.08173), high p-value (0.934), and negligible Sen's slope ($\sim 1.17e-07$) indicate that interannual variations in sea ice do not show a consistent increasing or decreasing pattern. This suggests that while sea ice concentration is clearly declining in the long term, the rate of change from one year to the next has remained statistically stable. 16

CWT - Sea Ice Concentration

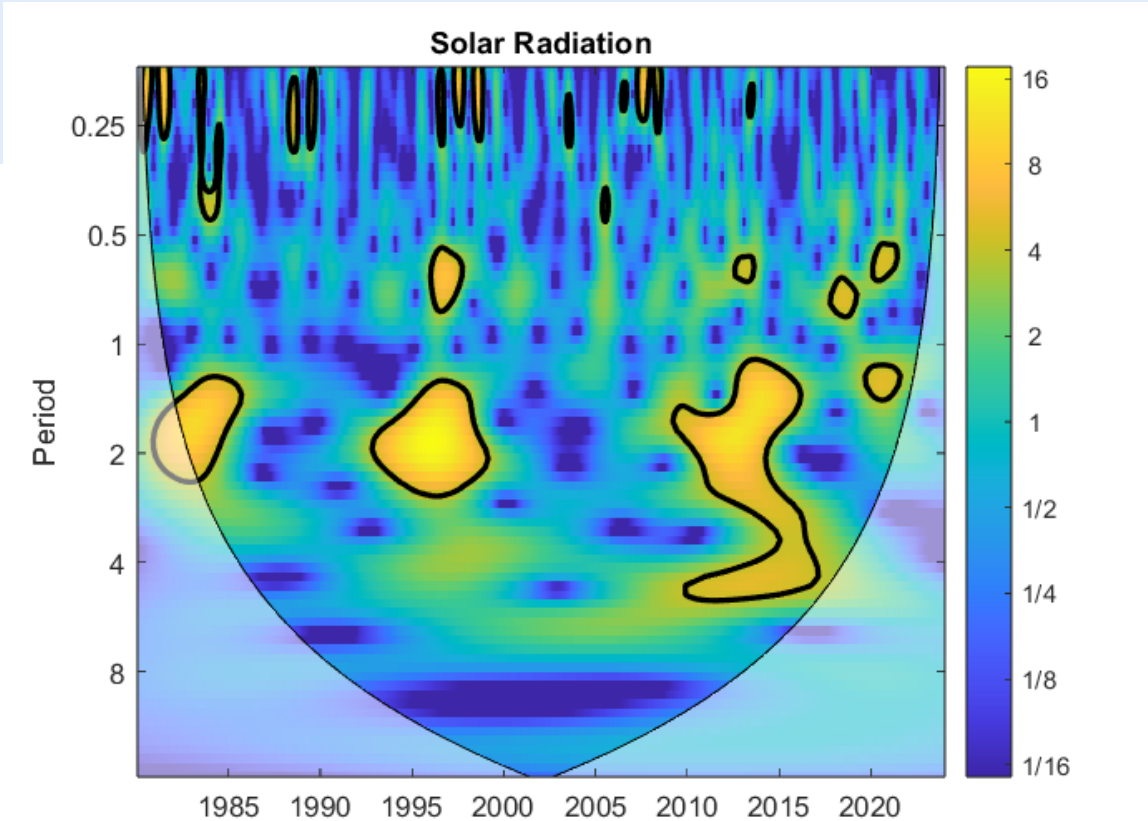


The Sea Ice Concentration CWT plot (likely representing a large-scale average) shows distinct episodes of variability. A strong interannual signal is present in the $\sim 1.5\text{--}2.5$ year band from approximately 1992 to 2000, with a particularly intense core around 1994–1998. Later in the record, another significant area of power emerges in a longer $\sim 3\text{--}5$ year period band, from roughly 2008 to 2018; the longer period components (around 4–5 years) of this signal towards 2018 approach the cone of influence and should be interpreted with some caution. Intra-annual variability (<1 year), particularly in the $\sim 0.5\text{--}0.75$ year band, is also notable in several episodes: around 1988–1993, 1998–2000, and 2005–2010, with a smaller patch around 2013–2015.

CWT

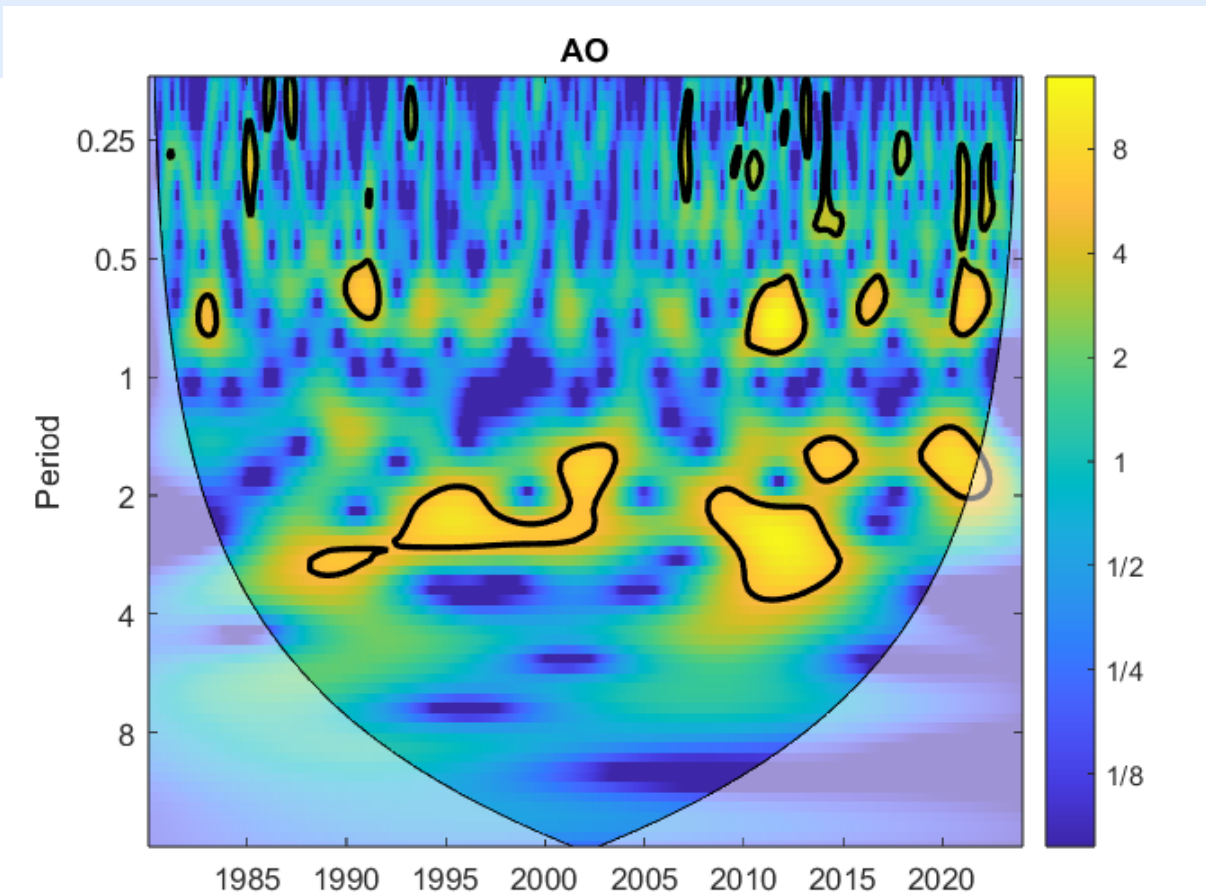


The NAO CWT plot indicates significant interannual variability, primarily in the $\sim 2\text{-}3$ year band. A strong episode of power in this band is evident from approximately 1992 to 2003. Another prominent region of significant variability in a similar $\sim 2\text{-}3$ year period emerges around 2008 and extends to near 2020, with the strongest core between 2010 and 2015. Intra-annual signals (<1 year) are also present in several distinct patches: around 1988-1990 (in the 0.25-0.5 year band), 1995-1998 (in the 0.5-0.75 year band), 2005-2008 (broadly in the 0.3-0.75 year band), 2010-2013 (in the 0.5-0.75 year band), and 2018-2020 (also in the 0.5-0.75 year band).

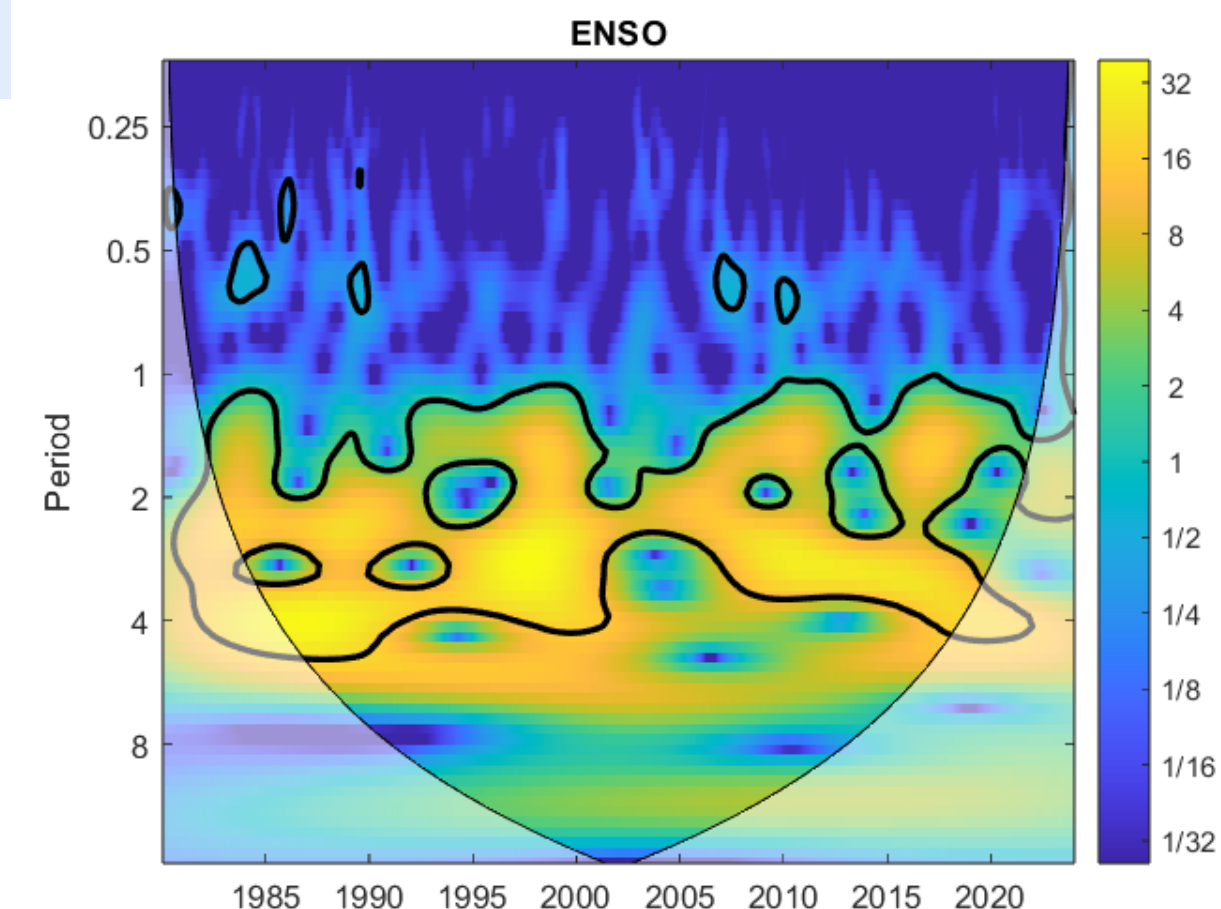


The Solar Radiation CWT plot highlights significant variability, particularly a very strong and broad interannual signal in the $\sim 1.5\text{-}5$ year band emerging around 2008 and persisting until approximately 2020. This feature shows considerable power across this range of periods, with a core often centered in the $\sim 2\text{-}4$ year band. This likely reflects variations associated with the solar cycle, although the ~ 11 -year cycle itself is too long to be fully resolved on this plot's period axis. Earlier in the record, significant power is observed in the $\sim 1.5\text{-}2.5$ year band from roughly 1993 to 2000. Another patch of significance is noted around 1982-1987 in the $\sim 1\text{-}2$ year band, with the earliest part of this signal being close to the cone of influence. Intra-annual signals (<1 year) also show several distinct episodes of significance, for example, in the $\sim 0.25\text{-}0.5$ year band around 1988-1992 and 1995-1998, and in the $\sim 0.5\text{-}0.75$ year band around 2005-2008 and 2018-2020.

CWT

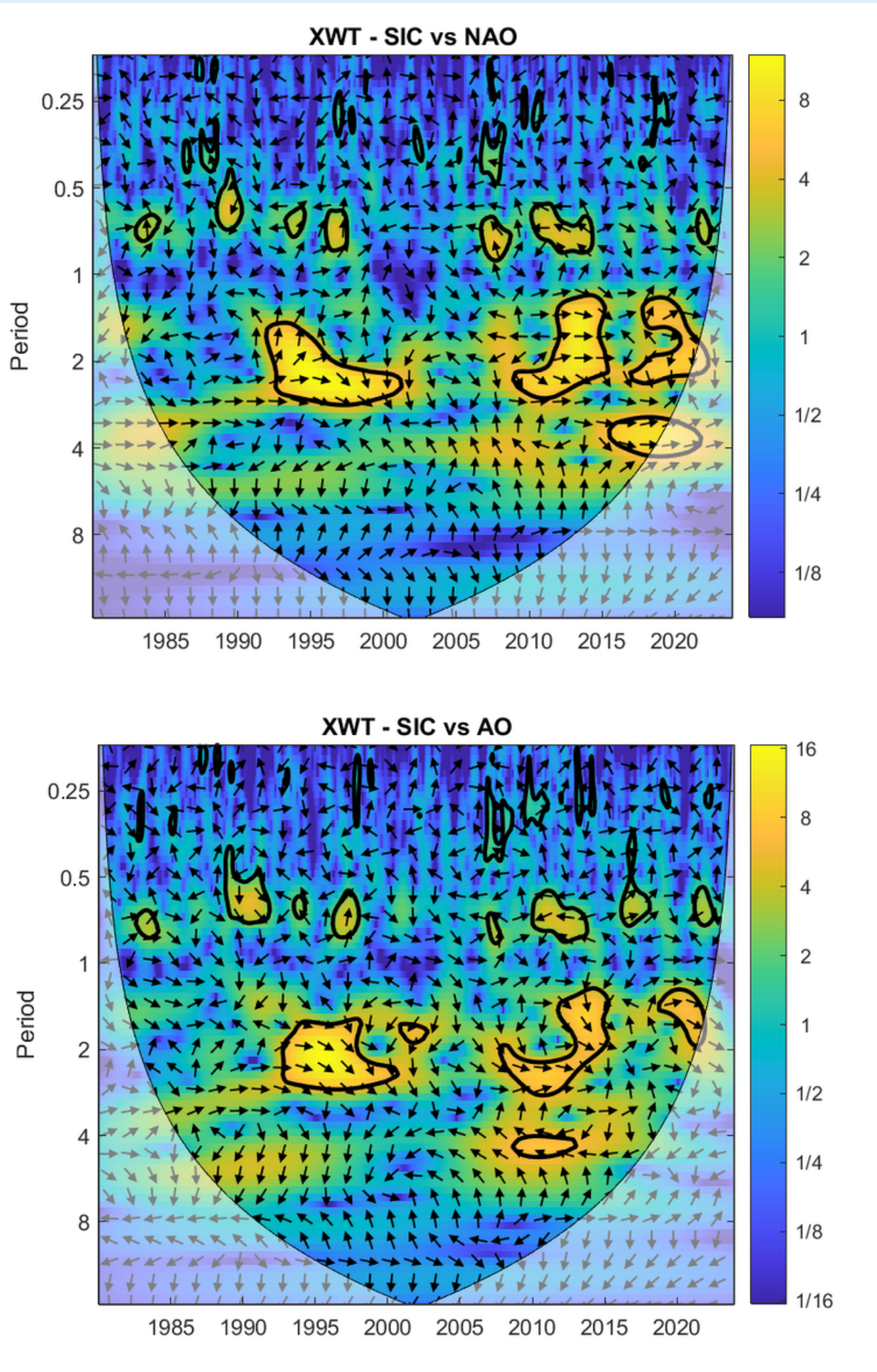


The AO CWT plot shows significant interannual variability, particularly in the $\sim 2-3.5$ year band. A strong episode is observed from approximately 1988 to 2003, centered around a 2-3 year period. Another significant, somewhat broader region of power in the $\sim 2-3.5$ year band emerges around 2008 and persists until roughly 2018, with its peak power shifting slightly towards longer periods within this band over time. Intra-annual variability (<1 year) is also present in several distinct, shorter-lived episodes: around 1985-1987 ($\sim 0.5-0.75$ year period), 1992-1994 (~ 0.5 year period), 2010-2013 ($\sim 0.5-0.75$ year period), and 2018-2020 (around the 0.5 year period).



The ENSO CWT plot demonstrates characteristic strong and persistent interannual variability, primarily concentrated in the $\sim 1.5-4$ year period band throughout the entire record (within the cone of influence). This broad band of power is a hallmark of ENSO. Within this, there are notable intensifications that often align with strong El Niño/La Niña events: for instance, a strong signal in the $\sim 2-4$ year range from the early 1980s to the mid-1990s (encompassing events like 1982-83, 1986-88, 1991-92). Power is also particularly significant around the $\sim 1.5-3$ year period from roughly 1997-2002 (capturing the strong 1997-98 El Niño) and again from 2008-2018 (including the 2009-10 and 2015-16 El Niño events). Shorter-lived intra-annual signals (<1 year) show intermittent significance, for example, around 1985-1988, 1992-1994, and 2005-2008, often in the $\sim 0.5-0.75$ year band.

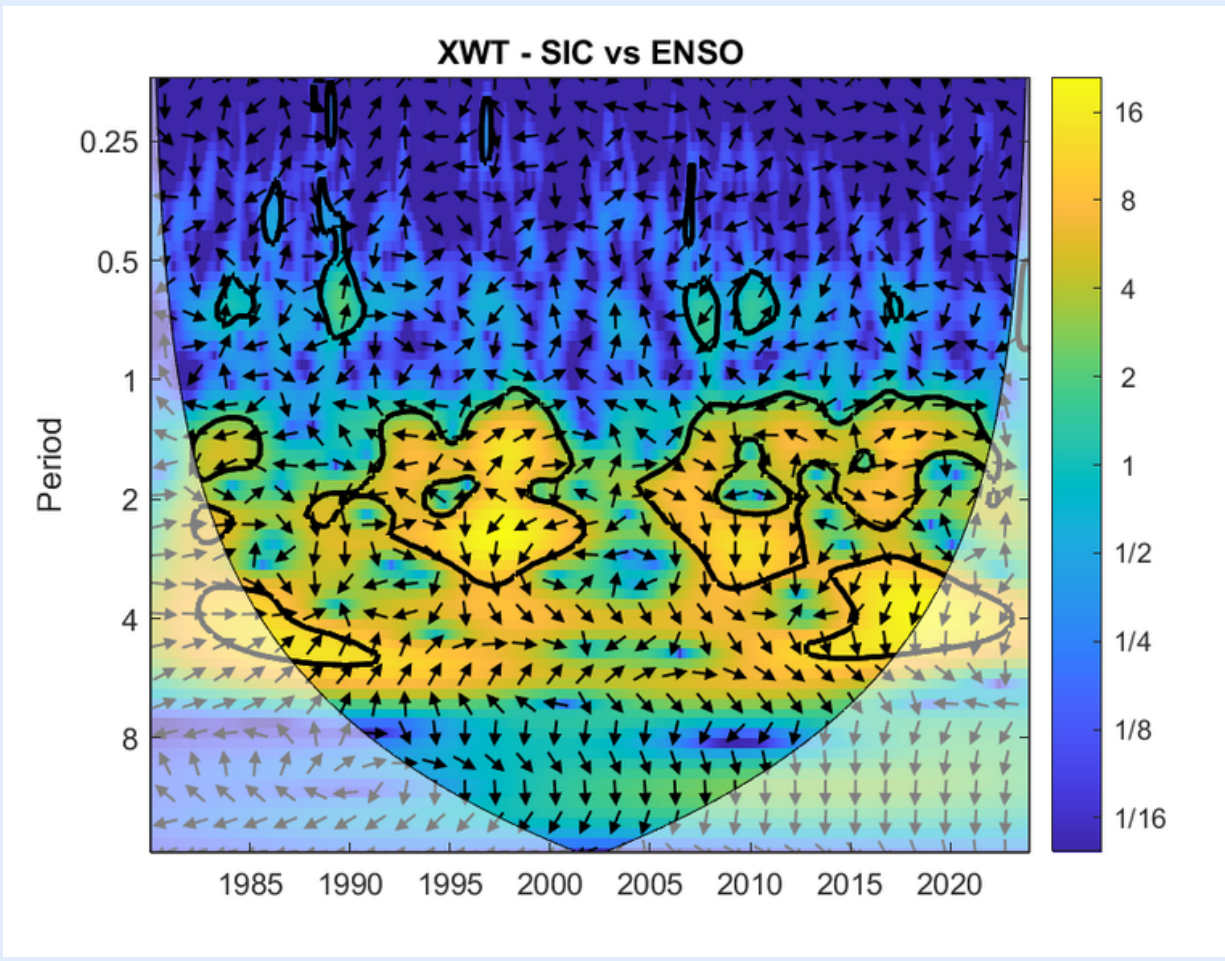
XWT



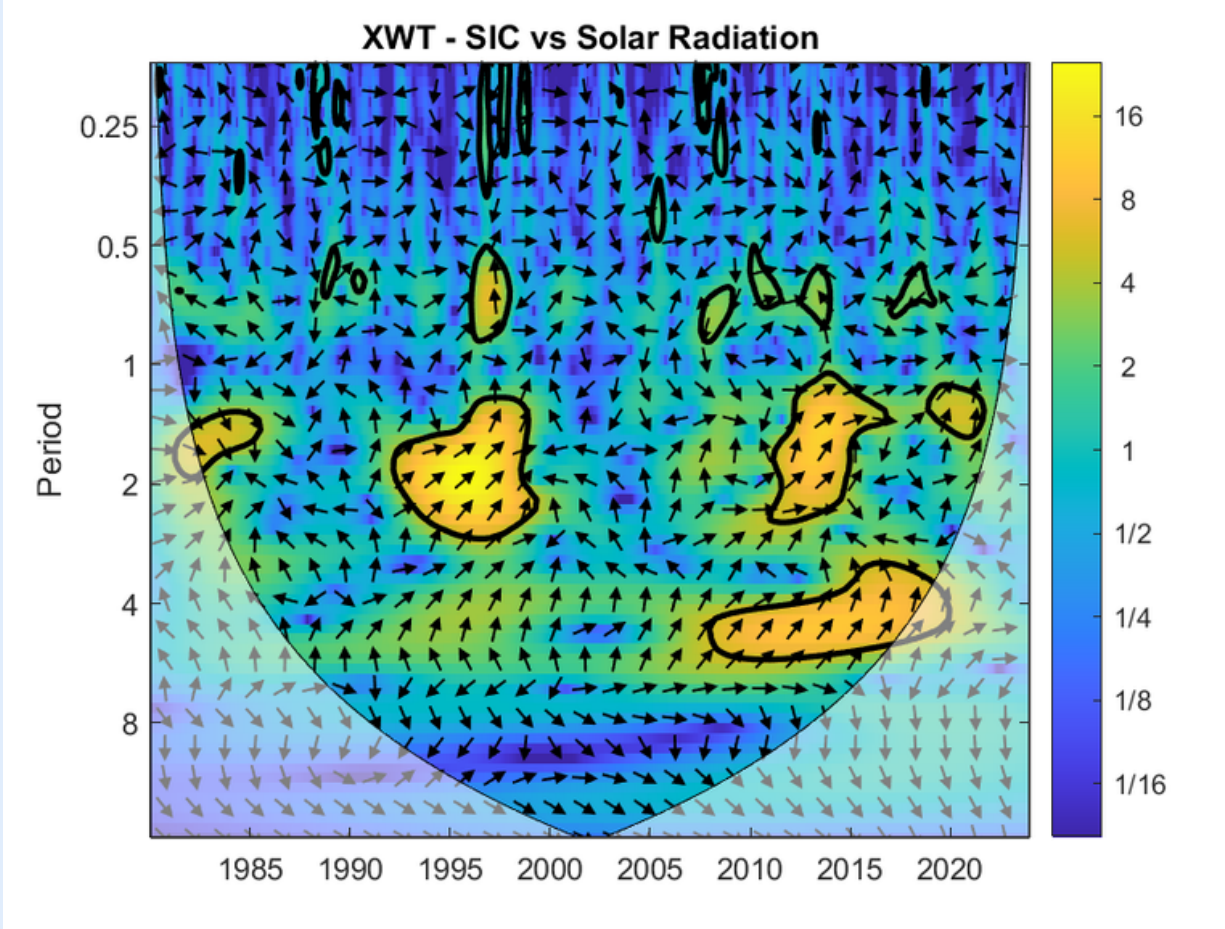
- This plot reveals that Sea Ice Concentration (SIC) and the North Atlantic Oscillation (NAO) share significant common power intermittently. A strong connection is visible in a 2-4 year period band from approximately 1990 to 2000, and again around 2010–2015 at a shorter 1-2 year period. The arrows are consistently pointing left, indicating a strong anti-phase relationship. This means a positive NAO phase is powerfully linked to a decrease in sea ice during these specific times. The intermittent nature suggests the NAO's strong influence is not constant over the entire record.

The shared power between SIC and the Arctic Oscillation (AO) is concentrated in distinct, high-frequency events. The most powerful common variability occurred around 1995–2000 and again from 2010–2015, both centered on a 2-year cycle. During these periods, the relationship was strongly anti-phase (left-pointing arrows), meaning a positive AO phase was dynamically linked to a reduction in sea ice. This highlights that while the correlation may be intermittent (as seen in WTC), when the connection is active, it drives significant shared variance between the two phenomena.

XWT

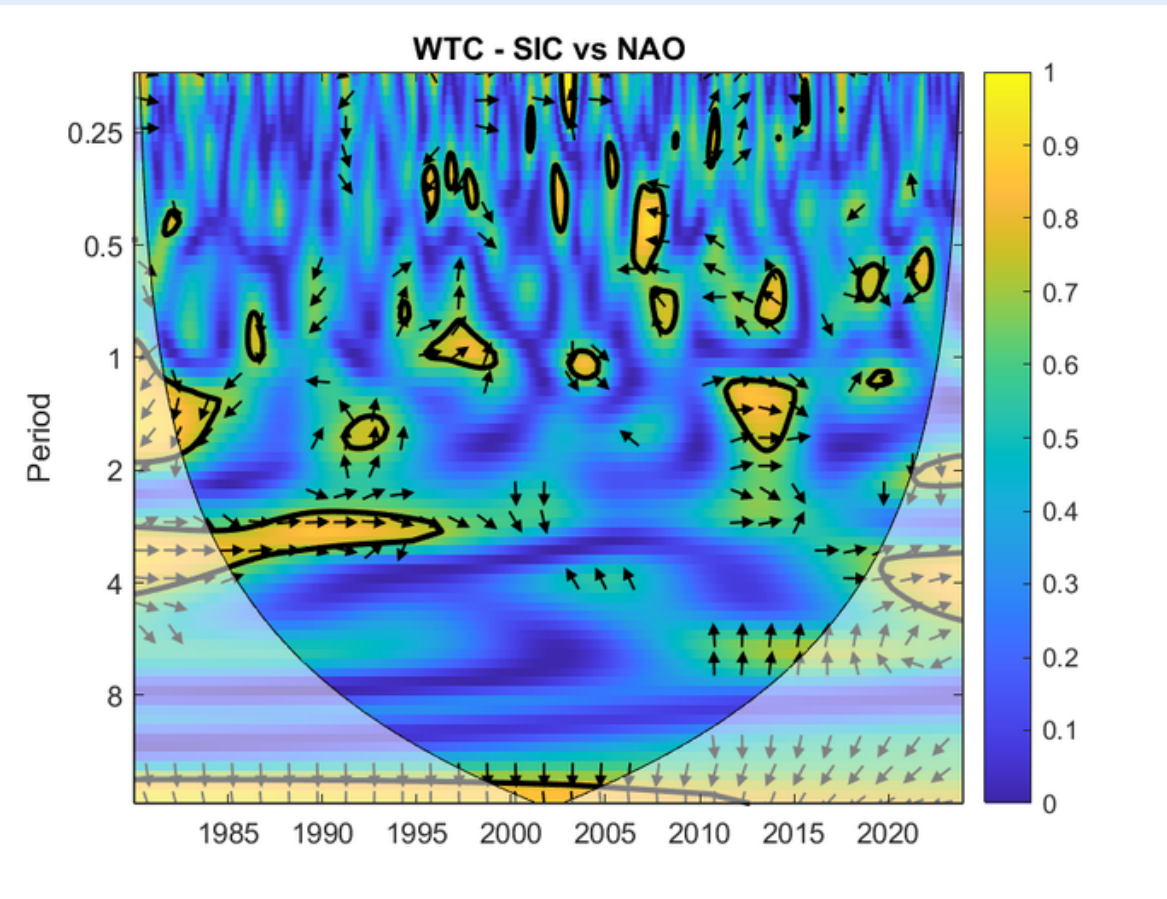


This plot reveals a remarkably broad and sustained region of shared power between SIC and ENSO. From approximately 1990 to 2015, there is a large, significant area of high power spanning the 2-8 year period band. The phase arrows are consistently pointing left, indicating a stable and powerful anti-phase relationship. This suggests that the variability linked to El Niño and La Niña events has a strong, persistent, and large-scale influence on Arctic sea ice fluctuations over multiple decades.

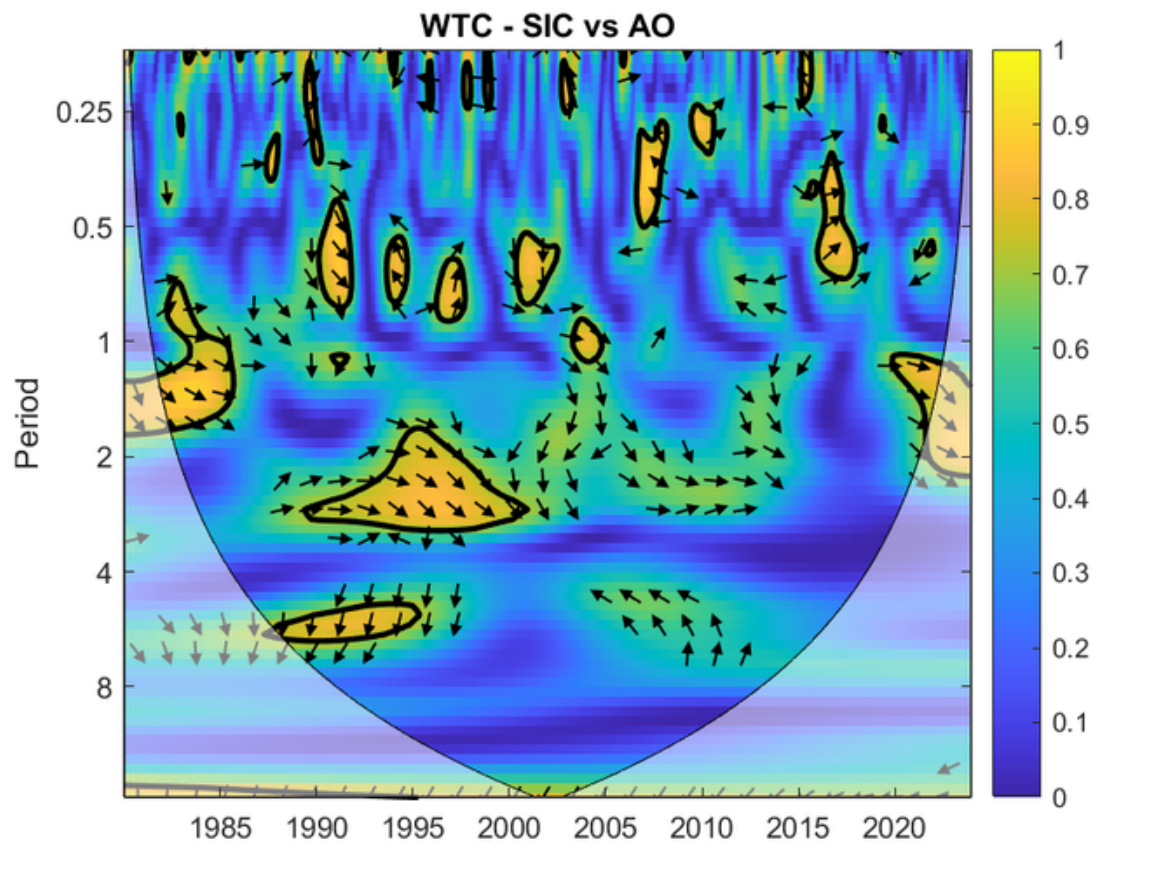


There is a very strong and significant common power between SIC and Solar Radiation, particularly after 2005. A powerful anti-phase relationship (left-pointing arrows) is evident in the ~4-year period band from 2005 to 2020. This physically intuitive result shows that periods of higher solar radiation are associated with strong decreases in sea ice. A weaker, but still significant, 2-year cycle also existed around 1995-2000. The strengthening of this connection in recent decades highlights the growing impact of solar energy cycles on sea ice variability.

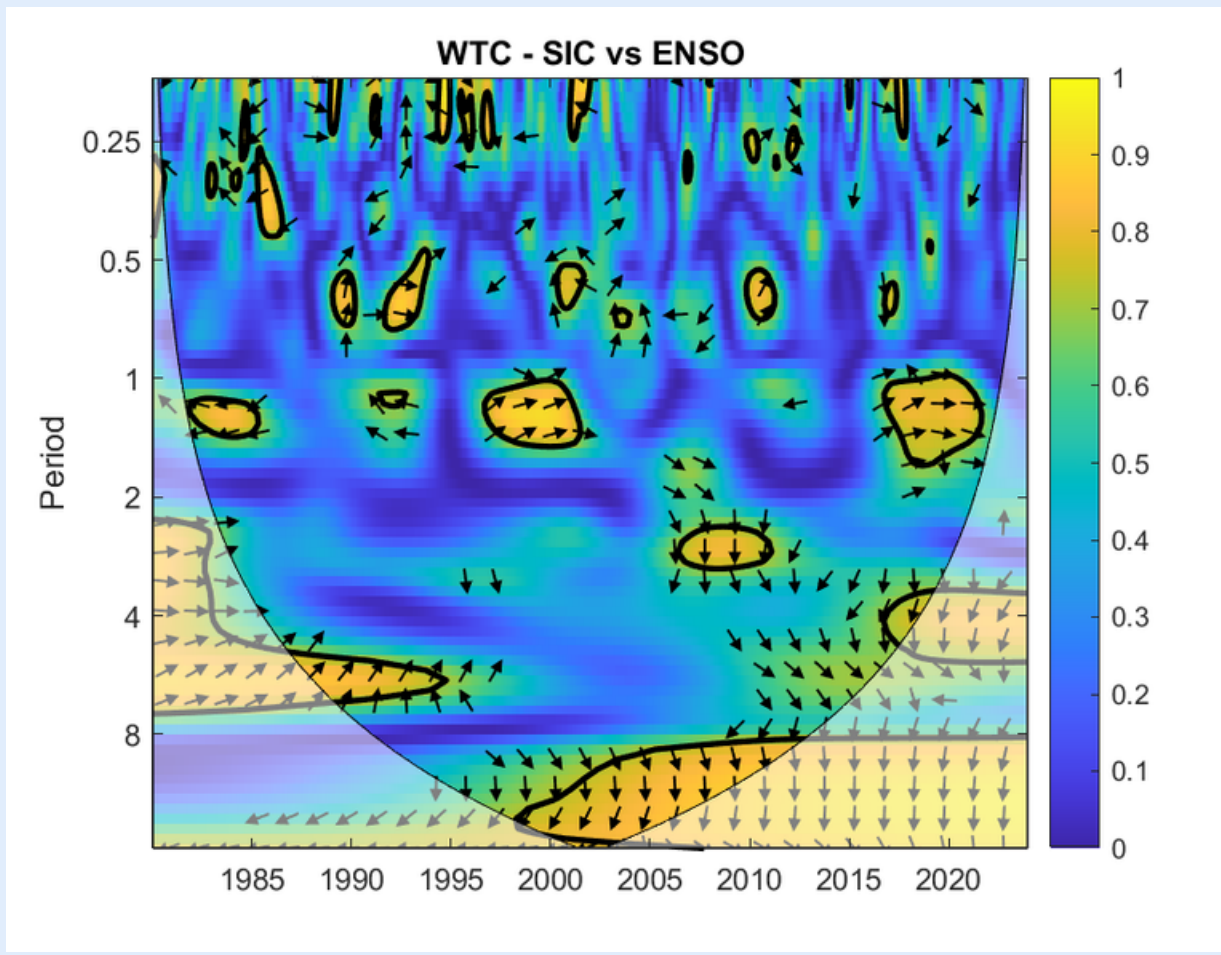
WTC



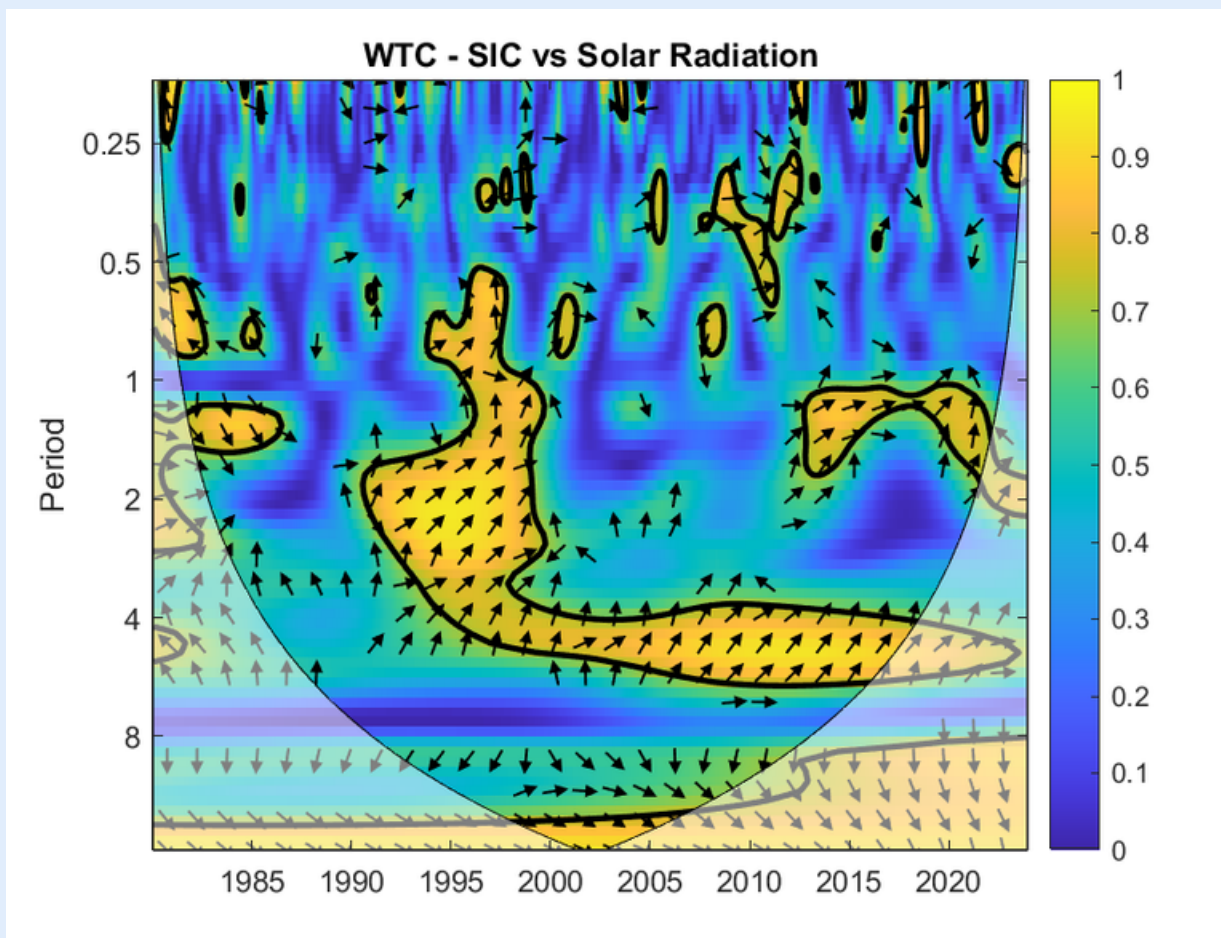
This plot highlights a distinct regime shift in the SIC-NAO relationship. An exceptionally strong and stable anti-phase correlation existed in a narrow ~3-year band from the mid-1980s until the late 1990s. During this time, the link was highly consistent, with a positive NAO reliably corresponding to lower sea ice. However, after the year 2000, this stable, long-lasting correlation breaks down and is replaced by much more sporadic and short-lived connections at different frequencies.



The coherence between SIC and the Arctic Oscillation (AO) is significant but episodic, occurring in distinct time-frequency windows. A notable anti-phase correlation exists in the 2-3 year band during the 1990s and again in a 4-6 year band from roughly 2005 to 2012. The arrows pointing left confirm that a positive AO phase is correlated with lower sea ice within these specific periods. This pattern suggests the AO's influence on sea ice is not constant, but rather "switches on" at different timescales in different decades.



The influence of the El Niño-Southern Oscillation (ENSO) on Arctic SIC is also significant but intermittent. A strong anti-phase correlation is visible at a 2-3 year period from about 2005 to 2012, where the upward-pointing arrows indicate that ENSO leads the changes in SIC. This suggests a teleconnection where tropical Pacific conditions impact Arctic ice a few months later. Another significant anti-phase link is present at a longer 4-8 year period in the 1990s, indicating that the nature of the ENSO-Arctic connection changes over time.



This plot shows an exceptionally strong and persistent correlation between SIC and Solar Radiation. A vast region of high coherence (yellow, close to 1) spans from the early 1990s to around 2015, covering the 2-8 year period band. The relationship is consistently anti-phase (left-pointing arrows), confirming that higher solar radiation is reliably linked to lower sea ice. The sheer breadth and strength of this coherence suggest that solar radiation is a fundamental and stable driver of multi-year sea ice variability. This stable correlation is one of the most dominant features across all the analyses.



Causality

Test for Stationarity because Granger causality tests require stationary time series (i.e., mean and variance don't change over time)

Granger causality doesn't mean true cause-effect in a physical sense. Instead, it tests whether past values of one time series contain information that helps predict future values of another.

```
grangercausalitytests(df[[target, predictor]], maxlag=12, verbose=False)
```

For each lag from 1 to 12:

- The test checks if including the past k months (lag) of the predictor improves the prediction of the target.
- It performs an F-test or Chi-squared test for significance.

Causality



Lag	NAO → SIC		AO → SIC		ENSO → SIC		Solar Radiation → SIC	
	p-value	✓/✗	p-value	✓/✗	p-value	✓/✗	p-value	✓/✗
1	0.294	✗	0.348	✗	0.4852	✗	0.0007	✓
2	0.0886	✗	0.2857	✗	0.2052	✗	0.0003	✓
3	0.0724	✗	0.431	✗	0.1922	✗	0.0001	✓
4	0.1056	✗	0.2771	✗	0.2597	✗	0.0003	✓
5	0.0669	✗	0.081	✗	0.2053	✗	0.0008	✓
6	0.0993	✗	0.0167	✓	0.2966	✗	0.0013	✓
7	0.0142	✓	0.0175	✓	0.4032	✗	0.002	✓
8	0.0147	✓	0.0282	✓	0.4806	✗	0.0081	✓
9	0.0205	✓	0.039	✓	0.4213	✗	0.0201	✓
10	0.034	✓	0.0483	✓	0.4894	✗	0.0493	✓
11	0.0055	✓	0.0279	✓	0.5356	✗	0.1766	✗
12	0.0109	✓	0.029	✓	0.4317	✗	0.3141	✗

Causality

Significance threshold used: $p < 0.05$



1. NAO → SIC

- Significant influence from Lag 7 to Lag 12, with lowest p-value at Lag 11 ($p = 0.0055$).
- Interpretation: The North Atlantic Oscillation shows a delayed impact on sea ice concentration, influencing SIC significantly after a lag of about 7 months or more.
- Possible Reason: The delayed response might be due to atmospheric circulation patterns gradually modifying Arctic conditions.

2. AO → SIC

- Significant influence from Lag 6 to Lag 12.
- First significant lag appears earlier than NAO (Lag 6) with $p = 0.0167$, and consistently significant through Lag 12.
- Interpretation: The Arctic Oscillation has a slightly earlier and sustained effect on SIC, which is expected as AO directly influences Arctic pressure and temperature anomalies.
- AO appears stronger and more consistently linked to SIC than NAO.

3. ENSO → SIC

- No significant influence at any lag.
- All p-values are above 0.19, with most > 0.4 .
- Interpretation: The El Niño–Southern Oscillation (ENSO) does not Granger-cause Arctic sea ice concentration in this dataset.
- Note: ENSO may still have indirect or lagged teleconnection effects not captured in this direct linear causality test.

4. Solar Radiation → SIC

- Strong and consistent significant influence from Lag 1 to Lag 10.
- Very low p-values (e.g., 0.0001 at Lag 3), indicating a strong causal relationship.
- Influence becomes non-significant after Lag 10.
- Interpretation: Changes in solar radiation have an immediate and powerful effect on sea ice, especially at short-term (monthly) lags.²⁶
- Reflects the direct thermodynamic effect of solar energy on sea ice melt/growth.

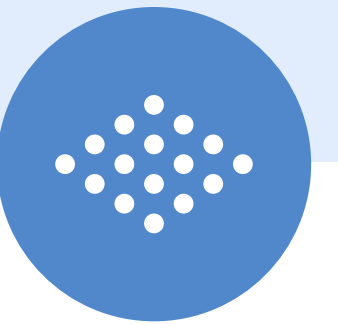
Conclusion

- Statistically significant WTC values >0.7 and XWT power SIC with Surface Solar Radiation Downwards (SSRD) across a interannual spectrum ($\sim 2\text{-}6$ years), particularly during the 1990–2015 period.
- WTC and XWT analyses identify statistically significant ($p < 0.05$) coherence and power btw Arctic SIC and ENSO, particularly on $\sim 2\text{-}4$ year and ~ 8 -year periodicities.
- WTC and XWT analyses statistically significant ($p < 0.05$) coherence and power btw Arctic SIC and both the AO and NAO. These significant relationships are most prominent within interannual frequency band periods of $\sim 2\text{-}4$ years and intermittently in the quasi-decadal band $\sim 4\text{-}8$ years.



References

- 
1. Swathi, M., Kumar, A., & Mohan, R. (2023). Spatiotemporal evolution of sea ice and its teleconnections with large-scale climate indices over Antarctica. *Marine Pollution Bulletin*, 188, 114634.
 2. Wang, Z., Li, Z., Zeng, J., Liang, S., Zhang, P., Tang, F., ... & Ma, X. (2020). Spatial and temporal variations of Arctic sea ice from 2002 to 2017. *Earth and Space Science*, 7(9), e2020EA001278.
 3. Yadav, J., Kumar, A., Srivastava, A., & Mohan, R. (2022). Sea ice variability and trends in the Indian Ocean sector of Antarctica: Interaction with ENSO and SAM. *Environmental Research*, 212, 113481.



**THANK
YOU!**

